Available online at www.sciencedirect.com
ScienceDirect
Journal of Hazardous Materials 143 (2007) 296–302
Journal of Hazardous Materials
www.elsevier.com/locate/jhazmat

Characteristics of equilibrium, kinetics studies for adsorption of fluoride on magnetic-chitosan particle

Wei Ma*, Fei-Qun Ya, Mei Han, Ren Wang

Department of Chemistry, College of Chemical Engineering, Dalian University of Technology, Dalian 116023, China

Received 3 May 2006; received in revised form 8 September 2006; accepted 8 September 2006
Available online 16 September 2006

Abstract

The magnetic-chitosan particle was prepared and characterized by the SEM, XRD, FT-IR and employed as an adsorbent for removal fluoride from the water solution in the batch system. The Langmuir isotherms, Bradley's isotherm, Freundlich isotherm and Dubinin–Kaganer–Radushkevich (DKR) isotherm were used to describe adsorption equilibrium. The kinetic process was investigated using the pseudo-first-order model, pseudo-second-order model and intra-particle diffusion model, respectively. The results show that the magnetic-chitosan particle is amorphous of irregular clumps in the surface with groups of RNH_2, RNH_3, Fe–O, etc. Bradley's equation and two-sites Langmuir isotherms were fitted well with the adsorption equilibrium data; the maximal amount of adsorption of 20.96–23.98 mg/l and free energy of 2.48 kJ/mol were obtained from the Bradley's equation, two-sites Langmuir isotherm and DKR modeling, respectively. The pseudo-second-order with the initial adsorption rate 2.08 mg/g min was suitable to describe the kinetic process of fluoride adsorption onto the adsorbent. In overall, the major mechanism of fluoride adsorption onto the heterogeneous surface of magnetic-chitosan particle was proposed in the study.

Keywords: Magnetic-chitosan; Removal fluoride; Adsorption isotherm; Kinetic

1. Introduction

The removal of fluoride from water is one of the most important issues due to the effect on human heath and environment. But as a necessary dilute element in human body, fluoride in drinking water may be beneficial or detrimental depending on its concentration [1]. The optimum fluoride level in drinking water for general good health set by World Health Organization (WHO) is considered to be less than 1.5 mg/l. Recently, removal fluoride from groundwater and waste water has been paid more attention in some literatures by the difference technology. For example, adsorption and biosorption [2–6], chemical precipitation including electrocoagulation/flotation process [7], membrane process such as reverse osmosis, nano-filtration and electrodialysis and Donnan dialysis [8–12] and others integrated process [13,14] were demonstrated effective method for removal fluoride. Each of the technology has been found to be limited, since the membrane processes often have high operational costs and the chemical precipitation may generate secondary wastes [7,9,10]. Among of these methods, adsorption technology as economical and efficient method and producing high quality water has been widely studied [2,6]. In recent years, many new type or traditional adsorbents were tested in different conditions. For example, the active alumina were obtained by deferent methods has all been used for fluoride removal practice [15–18] and modified chitosan by several process were used as adsorbents in the separation of cations and anions [19–24]. To date, adsorbent of magnetic particle was reported very little, if any, to removal fluoride from water solution, whereas magnetic particle adsorbent with excellent and controllable properties can be developed to bio-separation and removal ions from even very dilute aqueous solutions [21–27]. The main advantages are that the adsorption process is possible to be easily and simply separated using the external magnetic field and the sorbents will be reused.

In present work, a magnetic-chitosan particle was prepared and employed to remove fluoride from synthesized water solution with analytical grade reagents NaF and deionized water. Effect of pH values range from 5 to 9 was studied in the batch system and the fluoride removal ration in the adsorption pro-

* Corresponding author. Tel.: +86 411 84706030; fax: +86 411 84781798.
E-mail address: mawei@dlut.edu.cn (W. Ma).

0304-3894/$ – see front matter © 2006 Elsevier B.V. All rights reserved.
doi:10.1016/j.jhazmat.2006.09.032

cess compared by the activated alumina and magnetic particle at some dosage 1 g/l. In order to better understand adsorption of fluoride characteristic depend on the analysis of the SEM, XRD and FT-IR, the Bradley's equation model, Langmuir equation, two-sites Langmuir isotherm and Freundlich isotherms were employed to evaluate the sorption process at pH near 7. The pseudo-first-order, pseudo-second-order and intra-particle diffusion kinetic model were also used to study the dynamic process of adsorption.

2. Materials and methods

2.1. Synthesis of adsorbent

The magnetic-chitosan particle was prepared by developing the coprecipitation methods. First, 13.6 g $FeCl_3{\cdot}6H_2O$ was dissolved into 86.4 ml deionized water and 0.579 mol/l of Fe^{3+} solution was obtained, then 10.0 g $FeSO_4{\cdot}(NH_4)_2SO_4{\cdot}6H_2O$ was added into 90 ml deionized water for confect the 0.283 mol/l of Fe^{2+} solution. Then the 10% NaOH solution was added to mixed solution while maintaining a molar ratio of Fe^{3+}:Fe^{2+} = 3:2 until pH value was close to 9, the colloid of ferric/ferrous oxides should be formed [19]. Then chitosan and solution of $CaCl_2$ were mixed well with the colloid of Fe_3O_4, Next 2% alginate was added into them at slowly stirring condition until the sol was formed. After that, the sol was washed by 50 ml deionized water for 5 times and air-dried, calcined 12 h at the temperature of 110–120 °C. Finally, the obtained solid particle with chitosan was milled and sieved using 0.15 mm standard griddles and the magnetic-chitosan particle was selected by 0.2–0.4 T Nd–Fe–B magnetic field, which was ready for adsorption experimental test. The chemical agents were purchased from Tianjin Chemical agent plant and Chitosan was provided by Dalian Chitosan Limited Company of China. The sample was characterized by an X-ray diffractometer (XRD) (PW-1830 Philips), which was equipped with a Copper anode generating Cu Kα radiation (λ = 1.5406 Å). The surface structure, morphology and the elements were measured by scanning electron microscope (SEM) (JSM-5600LV) and Fourier transform-infrared spectroscopy (FT-IR) (Avatar-360 Nicolet) was also conducted on the sample.

2.2. Adsorption characteristics

Batch adsorption studies were conducted by contacting ca. 0.1 g quantities of adsorbent with 100 ml of solution at varying fluoride concentrations (5–140 mg/l) in 250 ml Erlenmeyer flasks shaking for ca. 150 min, which had been shown in preliminary study to ensure equilibration to be reached. Temperature of the adsorption tests was 18–20 °C while the pH of the water solution was adjusted in the range of 5–9 which simulated the pH level in typical groundwater using 0.01 M HCl or 0.01 M NaOH. After shaking 90 min or needed time depend on the experimental aims, the suspension was subjected for centrifugation and the final fluoride ions concentration of the supernatant was determined using fluoride ions spectrophotometer. The effect of pH, adsorption isotherms were carried out in batch systems. The kinetic experiments were performed in the same system at initial fluoride concentration 100 mg/l at pH 7. The compared experiment of fluoride removal rate with activated alumina, which provided by Dalian Water Treatment Company in the fluoride initial concentration 5–40 mg/l were also tested. Adsorption values were calculated from the change in solution concentration using the equation [28]:

$$q = \frac{V(C_0 - C_e)}{W} \quad (1)$$

where q is the adsorption amount (mg/g or mmol/kg), C_0 and C_e the initial and final concentrations (mg/l or mmol/l), V the volume of solution (l) and W is the mass of biosorbent used (g or kg).

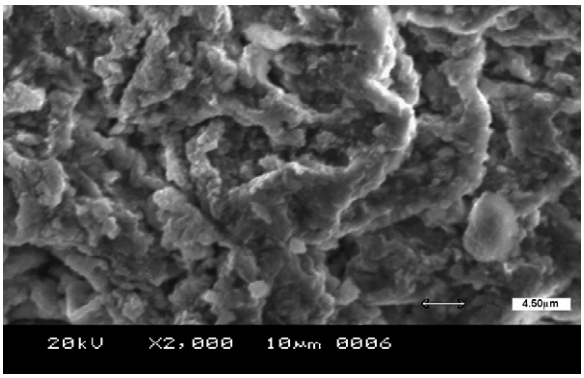

Fig. 1. SEM images of the adsorbent.

3. Results and discussion

3.1. The characteristics of the adsorbent

The magnetic-chitosan particle was milled into powders and examined by scanning electron microscope (SEM). SEM images show that the powder is irregular clumps (Fig. 1). The FT-IR results show in Fig. 2, as can be seen that peaks at ~2300 cm^{-1} and ~2920 cm^{-1} attribute to the stretching vibrations of RNH, RNH_2 in the chitosan. The peaks at 1620 cm^{-1}, 1420 cm^{-1} and 1042 cm^{-1} indicate the vibrations of group C=O and S–O, respectively. The peaks at 560–660 cm^{-1} attribute to the Fe–O bond vibration of Fe_3O_4. A broad band can be seen at 3400 cm^{-1}, which attributes to the hydroxyls [22–24,27]. The X-ray diffraction (XRD) pattern was used to identify the mor-

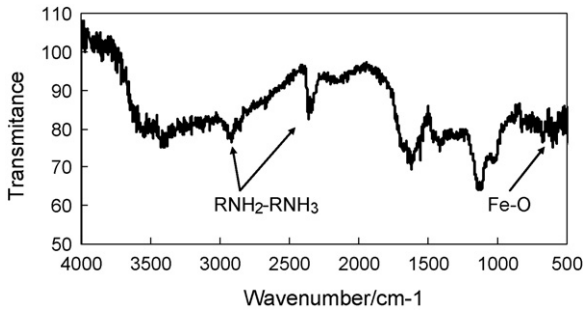

Fig. 2. FT-IR spectra of the magnetic-chitosan particle.

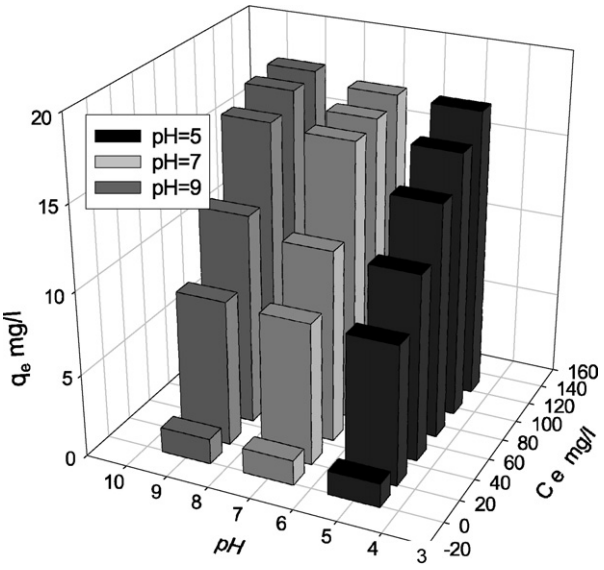

Fig. 3. Effect of pH for adsorbing process.

phological structure of the magnetic-chitosan particles; it cannot provide a quantitative peak to showing crystallization forms which suggests the magnetic particle is amorphous (figure not shown here).

3.2. The effect of pH and fluoride removal ratio in the adsorbent dosage 1 g/l

The results of pH effect were shown in Fig. 3, which indicates that better adsorption capacity q was obtained at pH 9 than others and there was no significant difference in adsorption capacity q of pH ranges from 5 to 9 at the constant fluoride initial concentration. The adsorption amounts strongly depend on the fluoride initial concentration, e.g. it is increasing from about 3 mg/g to 17 mg/g with corresponding initial concentration from 5 mg/l to 140 mg/l. It implies that the wide pH ranges suit to bonding the fluoride onto the absorbent, it due to less affected by the OH^- ions competition on the fluoride adsorption [5,6,16,18].

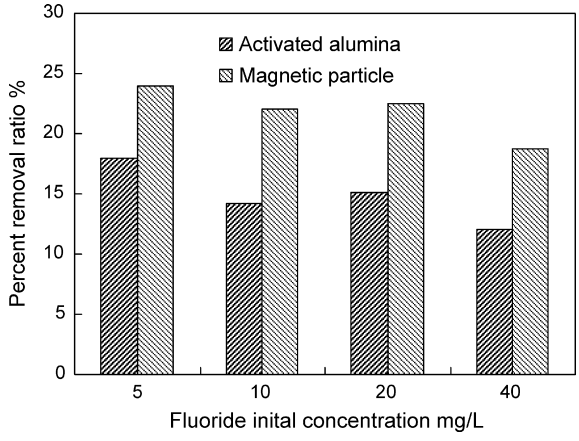

Fig. 4. Fluoride removal ratio in the adsorption process activated alumina and magnetic particle at adsorbent dose 1 g/l.

Fig. 4 shows the results of fluoride removal by the adsorption of activated alumina and magnetic particle at the 1 g/l dosage and pH 7 in the fluoride initial concentration from 5 mg/l to 40 mg/l. As can be seen that the fluoride removal ration from 24.0% and 18.0% down to 15.4% and 11% with the fluoride concentration increasing from 5 mg/l to 40 mg/l by the magnetic particle and activated alumina as adsorbents, respectively. The removal ratio is evidently depended on the adsorbents dosages [3,16,18] and more effect removal fluoride using the magnetic particle in the some conditions. It implies that the magnetic particle has lager adsorption amount per unit than the activated alumina [15,16,18] and was found to be superior to activated alumina in fluoride uptake in the water and wastewater treatment.

3.3. The adsorption equilibrium isotherm

In this work, the Langmuir isotherm, two-sites Langmuir isotherm, Bradley's equation and Freundlisch isotherm which expressed in Eqs. (2)–(5), respectively, were used for modeling biosorption equilibrium data. The details of the above isotherm are available in the literature [3,4,16,21,28,29]:

$$q_e = \frac{q_{max} b C_e}{1 + b C_e} \tag{2}$$

$$q_{2e} = \frac{q_1 b_1 C_e}{1 + b_1 C_e} + \frac{q_2 b_2 C_e}{1 + b_2 C_e} \tag{3}$$

$$q_e = \frac{q_{max} (K C_e)^m}{(1 + K C_e)^m} \tag{4}$$

$$q_e = k {C_e}^{1/n} \tag{5}$$

where q (q_e, or q_{2e}) is the amount of adsorbed fluoride ion per unit weight of biosorbent, q_{max} the maximum amount of adsorbate per unit weight of biosorbent (mg/g) and C_e is the remaining or equilibrium fluoride ion concentration in bulk solution (mg/l). The magnitude of b reflects the slope of the adsorption isotherm which is a measure of adsorption affinity coefficient (mg^{-1}). The K is a constant that is related to a Langmuir isotherm affinity (mg^{-1}) and m is a fitting exponent in the Bradley's equation model. The k (l/g) and $1/n$ are adsorption constants of Freundlich isotherm; q_1 and q_2 are the maximum capacity of the surface adsorbents sites 1 and 2 in the two-sites Langmuir isotherm (mg/g), and the total maximum capacity is $(q_1 + q_2)$ (mg/g); b_1 and b_2 are the corresponded affinity coefficients in the two-sites Langmuir isotherm (mg^{-1}). Using above provided isotherm fit the experimental data at pH of 7.0 ± 0.2, the results were shown in Fig. 5 and Table 1.

By comparing the correlation coefficients R^2 values and errors, we can see the correlation coefficients are more than 0.95 and the error value of Freundlich isotherm is larger than 10%, others error value loss than 10%. The Langmuirs isotherm and Bradley's equation were better than the Freundlich isotherm. It implies the adsorption experimental data were fitted well by the Bradley's equation and the Langmiur isotherm of the fluoride adsorption on the magnetic-chitosan particle. The results of two-sites Langmuir and Bradley's isotherm are similar and better than the classical Langmiur isotherm. The two-site Lang-

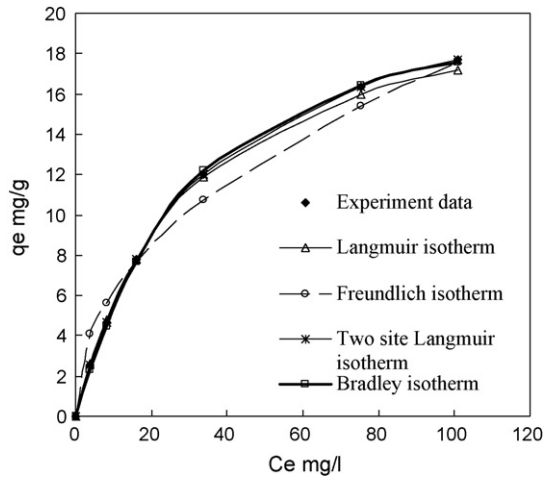

Fig. 5. The adsorption experimental data and modeling at pH 7.0 ± 0.2.

muir isotherm is modification of classical Langmuir isotherm model and is used to describe sorption on two sites with different binding energies. In this case, it indicates that there are different active groups with fluoride in the surface of the magnetic particle and q_2 value (15.08 mg/g) was close to two times value of q_1 (8.85 mg/g), which implies some groups have better bonding capacity then others. Considering the b_1 and b_2 values, which are closed, the adsorption intensity should be similar in all bonding site. The two sites capacity $q_1 + q_2$ is 23.98 mg/g more than the simple capacity 22.49 mg/g which obtained by classical Langmuir. As know that the Langmuir isotherm was based on the assumption of a structurally homogeneous adsorbent where all sorption sites are identical and energetically equivalent. So once the fluoride occupies a site, no further adsorption can take place at the same one. Where as from the two-sites Langmuir results, there different active sites in the adsorbent surface, so the heterogeneous monolayer adsorption was considered in the magnetic-chitosan particle. The sameness was obtained from the results of Bradley's isotherm model. The values obtained from the Bradley's equation were found to be, $q_{max} = 20.96$ mg/g and $n = 2.017$. The exponent value n suggests that the adsorption occurs on a heterogeneous surface [29], which is already stated above. This is consistence with an adsorption on an amorphous solid particle.

Table 1
Summary of equilibrium model application to fluoride adsorption onto magnetic particle at pH 7.0 ± 0.2

1. Langmuir isotherm constants	
q_{max} (mg/g)	22.49
b (mg^{-1})	0.0338
R^2	0.987
Δq (%)	9.23
2. Two-sites Langmuir isotherm constants	
q_1 (mg/g)	8.85
q_2 (mg/g)	15.08
b_1 (mg^{-1})	0.0288
b_2 (mg^{-1})	0.0289
R^2	0.990
Δq (%)	8.23
3. Bradley's equation constants	
q_{max} (mg/g)	20.96
K (mg^{-1})	0.996
n	2.017
R^2	0.994
Δq (%)	8.22
4. Freundlich isotherm constants	
K_f (l/g)	1.895
n	2.083
R^2	0.950
Δq (%)	17.30

3.4. Dubinin–Kaganer–Radushkevich (DKR) adsorption isotherm

Although two-site Langmuir and Bradley's isotherms provide that adsorption of fluoride onto the magnetic-chitosan particle was occurred at the monolayer region of heterogeneity surface and the maximum uptake value was obtained, it could not reveal the information of adsorption energy. The Dubinin–Kaganer–Radushkevich (DKR) equation has been widely used to explain energetic heterogeneity of solid surface at the monolayer region in micro-pores [30]. In order to better understand and clarify the adsorption process, equilibrium data were evaluated by DKR isotherm with Eq. (6):

$$\ln q_{ed} = \ln q_{md} - k\varepsilon^2 \tag{6}$$

where q_{ed} is the amount of fluoride adsorbed per unit weight of adsorbent (mmol/g), q_{md} the DKR monolayer adsorption capacity (mmol/g), k a constant related to adsorption energy (mol^2/kJ^2). The adsorption energy E (kJ/mol), can be obtained by Eq. (7):

$$E = -\frac{1}{\sqrt{-2k}} \tag{7}$$

It means energy for per mol adsorbate in transfer from infinity in solution to the surface. Where ε is Polanyi potential; can be obtained from Eq. (8):

$$\varepsilon = RT \ln\left(\frac{1}{C_e}\right) \tag{8}$$

where T is temperature (K), R the gas constant (J/mol K) and C_e is the equilibrium concentration of fluoride (mmol/l).

The q_{md} and k values of magnetic particle adsorption of fluoride were obtained by plotting $\ln q_{ed}$ versus ε^2 (Fig. 6) according to experimental data. The slope of line yields k (mol^2/kJ^2) and the intercept is equal to $\ln q_{md}$. The fitting results were presented in Table 2.

Table 2
Dubinin–Radushkevich parameters for fluoride on magnetic particle

Sample	Magnetic particle
T (°C)	17
q_m (mmol/g)	0.72 (13.68 mg/g)
k ($\times 10^{-8}$ mol^2/kJ^2)	6.27
R^2	0.934
$-E$ (kJ/mol)	2.84

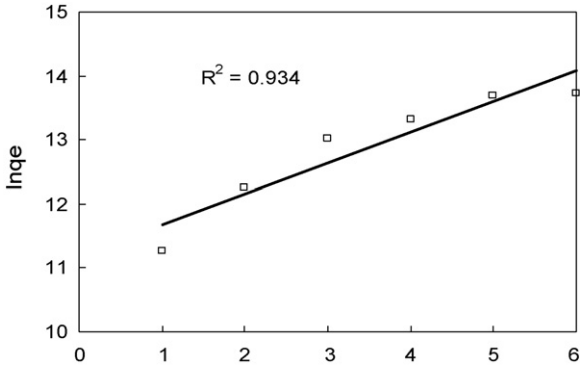

Fig. 6. Plot of $\ln q_e$ vs. ε^2 ($\times 10^{-8}$ mol^2/J^2) for Fluoride adsorption.

From Table 2 it can be seen DKR parameters correlation coefficient (R^2) is 0.934. The magnitude of free energy was used for estimating the type of adsorption [30,31]. The free energy E of 2.84 kJ/mol was obtained using Eq. (7). Since E values found in this work are less than 8 kJ/mol, the type of adsorption is physical adsorption due to weak Van Der Waals forces. The result is a good agreement with findings reported by Hu et al. [27] in which the physical adsorption of anionic hexachromium adsorption onto the magnetic particle. The max capacity are 0.72 mmol/g, i.e. 13.68 mg/g, which is lesser than the value from Langmuir and Bradley's isotherms; it may be due to the DKR modeling appropriate to the condition of lower initial concentration.

3.5. The adsorption kinetics

With regards to further adsorption characteristics of fluoride onto the magnetic-chitosan particle surface, the effect of contact time on the amount of fluoride adsorbed was examined at pH 7 and concentration of 100 mg/l of fluoride. The results presented in Fig. 7, as can be seen the maximum uptake of fluoride was observed at about 80–90 min. There was almost no further increase of adsorption after 90 min.

Several kinetic models have been applied to find out the adsorption mechanism [2,30–33]. The pseudo-first-order equation, pseudo-second-order equation and the intra-particle diffusion model with equations from (9) to (11) were employed to the kinetic analysis of fluoride onto magnetic particle, respectively:

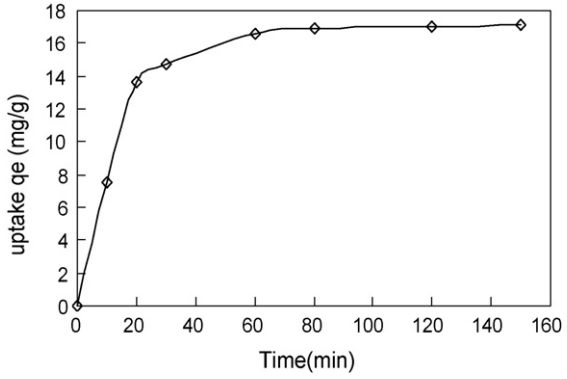

Fig. 7. Effect of reaction time to the adsorbing process.

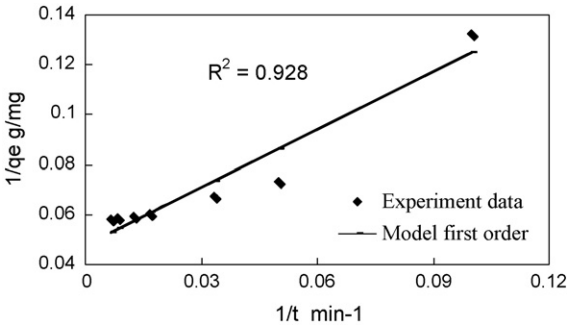

Fig. 8. The linear plot of $1/q_e$ vs. $1/t$.

$$\frac{1}{q_e} = \frac{k_1}{q_1}\frac{1}{t} + \frac{1}{q_1} \tag{9}$$

$$\frac{t}{q_e} = \frac{1}{k_2 q_2^2} + \frac{t}{q_2} \tag{10}$$

$$q_e = k_p t^{1/2} + C \tag{11}$$

where q_e (mg/g) is the uptake of fluoride at time t, q_1 (mg/g) the maximum adsorption capacity for pseudo-first-order, and k_1 (min^{-1}) is the pseudo-first-order rate constant for fluoride in adsorption process, respectively. The q_2 (mg/g) is the maximum adsorption capacity for the uptake and k_2 (min^{-1}) is the rate constant of fluoride in the pseudo-second-order adsorption process, the initial adsorption rate is $k_2 q_2^2$ (mg/g min). The k_p (mg/g min$^{0.5}$) is the intra-particle diffusion rate constant and C of adsorption constant is the intercept.

By plotting $1/q_e$ was versus $1/t$ according to pseudo-first-order model, a straight line with equation $1/q_e = 0.768(1/t) + 0.0479$ was obtained in Fig. 8 and related parameters are shown in Table 3. The correlation coefficient was given 0.928 and q_1 value was 20.88 mg/g, which closes to the obtained q_{max} from Langmuir isotherm and Bradley's equation.

Fig. 9 was obtained by plotting t/q_e versus t, in which the linear equation was $t/q_e = 0.0546t + 0.480$ and correlation coefficient was 0.997. The linearity of the plots implies the applicability of the pseudo-second-order kinetic equation for adsorption of fluoride onto magnetic-chitosan particle under

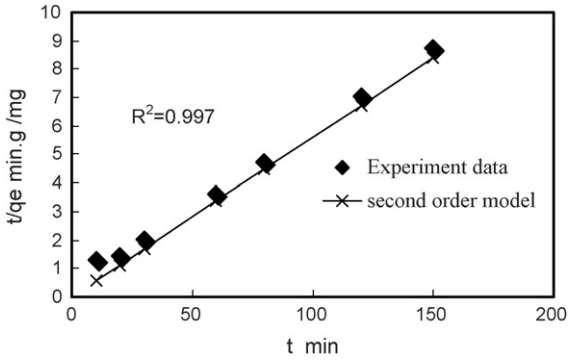

Fig. 9. The linear plot of t/q_e vs. t.

Table 3
The kinetic parameters of first-order, second and inter-particle model

Model	Rate constant	Adsorption constant (mg/g)	Coefficient R^2
First-order model	k_1 (min^{-1}): 16.03	q_1: 20.88	0.928
Second-order model	k_2 (mg/mg min): 6.21	q_2: 18.32	0.997
Intra-particle diffusion model	k_p (mg/g $min^{0.5}$): 1.31		0.770

experimental conditions. The parameters of k_2 and q_2 for the adsorption of fluoride were obtained from the slopes and intercepts of the pseudo-second-order plots and were given in Table 3.

The plots of q_t versus $t^{1/2}$ for the intra-particle diffusion model given in Eq. (11) were tested by fitting experimental data. Correlation coefficient for intra-particle diffusion value was 0.770. No plots were given for the intra-particle diffusion model due to their low coefficient, and the parameters calculated were presented in Table 3. It gives an indication of an intra-particle diffusion is not the rate-controlling step and others process may control the rate of adsorption [33].

The results show that the pseudo-second-order model was more approached describing the kinetic process of fluoride adsorption onto the magnetic-chitosan particle. The max capacity was less than the values from Langmuir isotherm and Bradley's equation, which may be due to the fluoride initial concentration was lower than the initial concentration previous experiment. The results agree with the literature [23], which has pointed out that as pseudo-second-order equation agrees controlling mechanism in the studies adsorption of Cu^{2+} onto chitosan. The adsorption of Fluoride onto the magnetic-chitosan particle may be considered to consist of two processes with initial adsorption rate 2.08 mg/g min was obtained.

As concerning adsorption characteristics of fluoride on the surface of the magnetic particle, the results of FT-IR of experimental sample show that the main groups are amino groups (RNH_2, RNH_3), Fe–O, etc., that is useful in determining adsorption of fluoride mechanism. The authors of literatures [19–21] have been noted the capacity of adsorption anions onto the chitosan depended on the amino groups, and Fan et al. [2] presented the ferric ions could act as a bridge to connect fluoride onto sorbent surface and enhance the adsorption of fluoride. The others researchers also indicated that metal oxides can be act with fluoride [3,5,17]. Therefore, in this study, it is reasonable to speculate that the fluoride is adsorption on the surface of the magnetic particle main acted with the –NH (RNH_2, RNH_3) and Fe–O groups by the physical forces. The fluoride ions may be in order disposed onto the groups of surface of magnetic particle by the unlikeness amount of fluoride ions.

In overall, the major mechanism of fluoride ions adsorption by the magnetic particle may be proposed schematic as in Fig. 10.

Although group of amine and metal oxides may be major acted role, it should be pointed out that the others groups also effect on the fluoride adsorption due to it is a surface complexation reaction. Regeneration studies demonstrated that the loading fluoride magnetic particle was recovered by 0.8–1% NaOH washing-water rinsing-heating and the reused sorbents adsorption capacity was achieved to 98–99% (data no show).

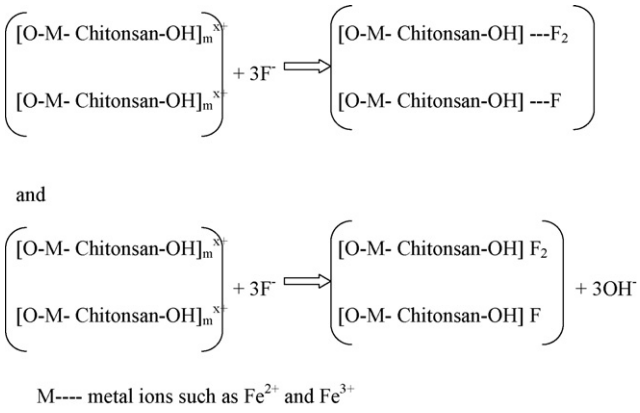

Fig. 10. Schematic description of adsorption mechanism.

The affect of co-exist ions such as chloride, phosphate, nitrate, sulphate, etc., anions and other cations, which were noted in literature [8–12,19,21,26], are also important for the further application in practice. Current work in our laboratory involves development of present study to address competition effects and extension to adsorption behaviors in multi-system.

4. Conclusion

Magnetic-chitosan particles were prepared by the coprecipitation methods and character using the SEM, XRD, and FT-IR, and characteristics of equilibrium, kinetics which used as adsorbents of defluoridation were tested. This work confirms that magnetic-chitosan particle is suitable adsorbent for the removal fluoride from water and waste water. The uptake is 20.96–23.98 mg/g and it is depended the fluoride initial concentration and the pH. The character of magnetic particle was analysis by the SEM, XRD, and FT-IR, which indicate that it is amorphous with the groups of RNH_2, RNH_3, Fe–O, etc. The two-sites Langmuir isotherm and Bradley's equation were fitted well with the experimental equilibrium data and noted that the adsorption of fluoride occurred at the heterogeneity surface by the physical adsorption due to the adsorption free energy was 2.48 kJ/mol, which obtained by the Dubinin–Kaganer–Radushkevich (DKR) model. The results of kinetic modeling show that the pseudo-second-order kinetic model was better described the time effect on the fluoride adsorption than the pseudo-first-order model and intra-particle diffusion model. It presented the rate determining step of fluoride adsorption onto the major sites of amino and Fe–O groups and it controlled by two processes with initial adsorption rate 2.08 mg/g min. These preliminary results warrant further investigations for application of magnetic particle in practice.

Acknowledgements

The authors gratefully acknowledge financial support received from the NSFC (29777011) and Education Department of China. Sincere thanks are given to the reviewers for their valuable comments to improve the paper.

Appendix A. Supplementary data

Supplementary data associated with this article can be found, in the online version, at doi:10.1016/j.hazmat.2006.09.032.

References

[1] World Health Organization (WHO), Guidelines for Drinking Water Quality, vol. 1, World Health Organization, Geneva, 1993, pp. 45–46.
[2] X. Fan, D.J. Parker, M.D. Smith, Adsorption kinetics of fluoride on low cost materials, Water Res. 37 (2003) 4929–4937.
[3] M.S. Onyango, Y. Kojima, O. Aoyi, E.C. Bernardo, H. Matsuda, Adsorption equilibrium modeling and solution chemistry dependence of fluoride removal from water by trivalent-cation-exchanged zeolite F-9, J. Colloid Interface Sci. 279 (2004) 341–350.
[4] Y.H. Li, S. Wang, X. Zhang, J. Wei, C. Xu, Z. Luan, D. Wu, Adsorption of fluoride from water by aligned carbon nanotubes, Mater. Res. Bull. 38 (2003) 469–476.
[5] A.K. Yadav, C.P. Kaushik, A.K. Haritash, A. Kansal, N. Rani, Defluoridation of groundwater using brick powder as an adsorbent, J. Hazard. Mater. B128 (2006) 289–293.
[6] S.V. Mohana, S.V. Ramanaiah, B. Rajkumar, P.N. Sarma, Biosorption of fluoride from aqueous phase onto algal Spirogyra IO1 and evaluation of adsorption kinetics, Biores. Technol. (2006) (online available).
[7] M.M. Emamjomeh, M. Sivakumar, An empirical model for defluoridation by batch monopolar electrocoagulation/flotation (ECF) process, J. Hazard. Mater. B131 (2006) 118–125.
[8] C. David, M.C. Herbert, 65,000 GPD fluoride removal membrane systems in Lakeland, California, USA, Desalination 117 (1998) 19–35.
[9] K. Hu, M.D. James, Nanofiltration membrane performance on fluoride removal from water, J. Membr. Sci. 279 (2006) 529–538.
[10] P.I. Ndiaye, P. Moulin, L. Domingwez, J.C. Millet, F. Charbit, Removal of fluoride from electronic industrial effluent by RO membrane separation, Desalination 173 (2005) 25–32.
[11] T. Ruiz, F. Persin, M. Hichour, J. Sandeaux, Modelisation of fluoride removal in Donnan dialysis, J. Membr. Sci. 212 (2003) 113.
[12] M. Hichour, F. Persin, J. Sandeaux, C. Gavach, Fluoride removal from waters by Donnan dialysis, Sep. Purif. Technol. 18 (2000) 1–11.
[13] N. Parthasarathy, J. Buffle, W. Haerdi, Combined use of calcium salts and polymeric aluminum hydroxide for defluoridation of wastewaters, Water Res. 20 (1986) 443–448.
[14] M. Hichour, F. Persin, J. Sandeaux, C. Gavach, Fluoride removal from by diluted solution by Donnan dialysis with anion-exchange membrane, Desalination 122 (1999) 53–62.
[15] L. Lv, J. He, M. Wei, D.G. Evans, X. Duan, Factors influencing the removal of fluoride from aqueous solution by calcine Mg–Al–CO_3 layered double hydroxides, J. Hazard. Mater. (2005) (online available).
[16] S. Ghorai, K.K. Pant, Equilibrium, kinetics and breakthrough studies for adsorption of fluoride on activated alumina, Sep. Purif. Technol. 42 (2005) 265.
[17] H. Lounici, D. Belhocine, H. Grib, M. Drouiche, A. Pauss, N. Mameri, Fluoride removal with electro-activated alumina, Desalination 161 (2004) 287–293.
[18] C.L. Yang, Dluhy, Electrochemical generation of aluminum sorbent for fluoride adsorption, J. Hazard. Mater. 94 (2002) 239.
[19] I.M.N. Vold, K.M. Vårum, E. Guibal, O. Smidsrø, Binding of ions to chitosan—selectivity studies, Carbohydr. Polym. 54 (2003) 471–477.
[20] E. Guibal, L. Dambies, C. Milot, J. Roussy, Influence of polymer structural parameters and experimental conditions on metal anion sorption by chitosan, Polym. Int. 48 (1999) 671–680.
[21] H. Yoshida, N. Kishimoto, T. Kataoka, Adsorption of strong acid on polyaminated highly porous chitosan: equilibria, Ind. Eng. Chem. Res. 33 (1994) 854–859.
[22] Y.C. Cheng, D.H. Chen, Magnetic chitosan nanoparticles: studies on chitosan binding and adsorption of Co(II) ions, React. Funct. Polym. 66 (2006) 335–341.
[23] Y.C. Chang, D.H. Chen, Preparation and adsorption properties of monodisperse chitosan-bound Fe_3O_4 magnetic nanoparticles for removal of Cu(II) ions, J. Colloid Interface Sci. 283 (2005) 446.
[24] E.B. Denkbas, E. Kilicay, C. Birlikseven, E. Oztuk, Magnetic chitosan microspheres: preparation and characterization, React. Funct. Polym. 50 (2002) 225–232.
[25] D.N. Williams, M. Chorny, B. Yellen, B. Fishbein, I. Stanley, J. Stachelek, O. Nyanguile, G. Friedman, Magnetic nanoparticle mediated gene and cell delivery, Mol. Therapy 11 (2005) S355.
[26] Z.G. Peng, K. Hidajat, M.S. Uddin, Selective and sequential adsorption of bovine serum albumin and lysozyme from a binary mixture on nanosized magnetic particles, J. Colloid Interface Sci. 281 (2005) 11–17.
[27] J. Hu, G. Chen, I.M.C. Lo, Removal and recovery of Cr(VI) from wastewater by maghemite nanoparticles, Water Res. 39 (2005) 4528–4536.
[28] W. Ma, J.M. Tobin, Development of multimetal binding model and application to binary metal biosorption onto peat biomass, Water Res. 37 (2003) 287–295.
[29] W.J. Weber Jr., F.A. DiGiano, Process Dynamics in Environmental Systems, Wiley-Interscience, New York, 1996.
[30] B.S. Krishna, N. Mahadevaiah, D.S.R. Murty, B.S. Jai Prakash, Surfactant immobilized interlayer species bonded to montmorillonite as recyclable adsorbent for led ions, J. Colloid Interface Sci. 271 (2004) 270–276.
[31] M. Yurdakoc, Y. Seki, S. Karahan, K. Yuedakoc, Kinetic and thermodynamic studies of boron removal by Siral 5, Siral 40, and Srial 80, J. Colloid Interface Sci. 286 (2005) 440–446.
[32] Y.S. Ho, G. Mckay, The kinetics of sorption of divalent metal ions onto sphagnum moss peat, Water Res. 34 (2000) 735–742.
[33] Z. Reddad, C. Gerente, Y. Andres, P.L. Cloirec, Adsorption of several metal ions onto a low-cost biosorbent: kinetic and equilibrium studies, Environ. Sci. Technol. 36 (2002) 2067–2073.